Lawrence Berkeley National Laboratory

Title

Quinoid-viologen conjugates: Redox properties and host-guest complex with cucurbiturils

Permalink

https://escholarship.org/uc/item/38j3d9n0

Authors

Chen, Z
Khoo, R
Garzón-Ruiz, A
et al.

Peer reviewed

Quinoid-viologen conjugates: redox properties and host-guest complex with cucurbiturils

Ziman Chen[a,b], Rebecca Khoo[b,f], Andrés Garzón-Ruiz[c], Chongqing Yang[b], Christopher L. Anderson[b,f], Amparo Navarro[d], Xu Zhang[e], Jian Zhang[b], Yongqin Lv[a,*] and Yi Liu[b,*]

[a]*Beijing Advanced Innovation Center for Soft Matter Science and Engineering, State Key Laboratory of Organic-Inorganic Composites, Beijing University of Chemical Technology, Beijing, 100029, China*

[b]*The Molecular Foundry, Lawrence Berkeley National Laboratory, Berkeley, California 94720, United States of America*

[c]*Department of Physical Chemistry, Faculty of Pharmacy, Universidad de Castilla-La Mancha, Cronista Francisco Ballesteros Gómez, Albacete 02071, Spain*

[d]*Department of Physical and Analytical Chemistry, Faculty of Experimental Sciences, Universidad de Jaén, Campus Las Lagunillas, Jaén 23071, Spain*

[e]*Jiangsu Engineering Laboratory for Environmental Functional Materials, School of Chemistry and Chemical Engineering, Huaiyin Normal University, Huaian, Jiangsu 223300, China*

[f]*Department of Chemistry, University of California, Berkeley, Berkeley, California 94720, United States of America*

Email address: yliu@lbl.gov (Y. Liu), *lvyq@mail.buct.edu.cn* (Y. Lv)

Dedicated to Prof. Sir J. Fraser Stoddart on the occasion of his 80th birthday

Abstract

Viologens are known as an excellent electron acceptor and a versatile supramolecular building block, the physical property of which can be tuned by varying the *N*-substitution. Herein, we present a class of unprecedented quinoid-viologen conjugates wherein a quinoidal unit is incorporated as part of an extended π-system of the viologen units through *N*-substitution. Such class of molecules show intriguing optical and electronic properties inherited from both the viologen and the quinoid constituents, displaying stronger electron accepting characters, visible absorption, reversible redox activity, modulated electrochromism, and characteristic binding towards Cucurbit[n]urils (n=7 and 8). This molecular design strategy points to a new direction to diversify viologens for functional electroactive materials and complex architectures.

*Keywords:* electron acceptor; host-guest complex; quinoid; redox active; viologen

1. Introduction

Viologens with the central di-quaternized 4,4'-bipyridyl structure have attracted broad interests for their exceptional redox properties [1]. Due to the electron deficiency endowed by the cationic characteristics of the pyridinium and the conjugated structure, viologen derivatives behave as strong electron acceptors with three readily accessible redox states and visible color changes, rendering interesting material properties for applications in electrochromic devices (ECDs), photocatalysis, redox flow batteries [2, 3], and more recently in electrochromic supercapacitors [4] and heat-shuttering windows [5]. Viologens have also become a cornerstone building block for supramolecular chemistry and molecular machinery [6-8]. Since its first incorporation in the famous tetracationic cyclobisparaquat macrocycle, also known as "blue box", in the foundational work by Stoddart and co-workers [9], numerous mechanically interlocked molecules with novel architectures and controllable switching properties have been demonstrated by the principle of electron donor-acceptor interactions [10-14] and radical templation [15-18]. It also behaves as a versatile guest to many macrocyclic hosts, such as crown ethers, cyclodextrins, and cucurbit[n]urils (CB[n]) [19-26]. Particular sized CBs, such as CB[7] [27, 28] and CB[8] [29-31], have shown tunable encapsulation behavior towards viologen derivatives in aqueous media as driven by various noncovalent interactions such as hydrophobic interactions and ion-dipole interactions, which form the basis for the synthesis of intricate molecular complexes [32-34] and advanced two-dimensional and three-dimensional architectures [35-37].

Despite the above attractions, viologens have poor absorption in the visible spectrum due to the relatively low degree of conjugation, a feature that significantly limits their utilization in photo-redox processes. This issue has

motivated the development of new molecular design strategies to improve both photophysical and electronic properties. The main approach has focused on the modification of the π-conjugated moiety of the bipyridinium by extending the core conjugation or ring fusion of the β-position of the pyridiniums (Scheme 1a) [38-42]. Another approach to varying the conjugation is through *N*-arylation, which can effectively extend the π-system to lower the frontier orbital energy gaps and tune the optical properties [32, 43]. Both core alternation and *N*-arylation however impose additional synthetic inconvenience compared to the prototypical *N*-alkyl viologens, the synthesis of which is facilitated by straightforward S_N2 reactions between 4,4'-bipyridine and alkyl halide precursors. Reaction systems that can introduce viologen units with extended conjugation through simple substitutive reactions are thus highly desirable [44].

para-Azaquinodimethane (AQM) ditriflates, such as **1** shown in Scheme 2, are novel quinoidal units [45-49] that have shown amenable S_N2 reactivity toward pyridyl units to afford pyridinium salts in high yields [46]. This reaction motif opens up the possibility to synthesize unexplored viologen derivatives that contain directly conjugated quinoid-viologen conjugates (Scheme 1c). Herein we describe the successful synthesis of such quinoid-viologen conjugates and demonstrate that their redox and optical properties are profoundly impacted due to the mixed aromatic-quinoid conjugation, rending them potent electron acceptors for narrow bandgap polymers. In addition, the supramolecular complexation of such viologens with CBs has also been investigated, which shows high dependence on the *N*-substituents and subtle difference in the binding motif compared to other known *N*-methyl and *N*-aryl viologens [50].
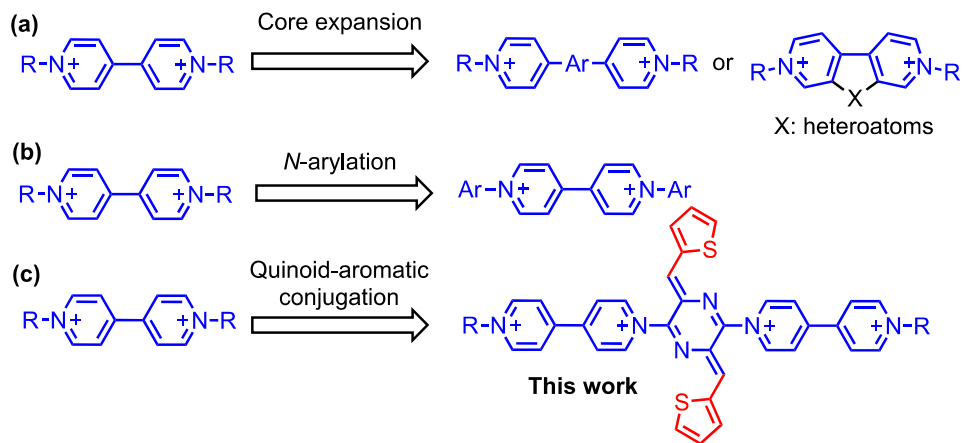

Scheme 1. Various conjugation strategies for tuning the electronic properties of viologens. **(a)** core expansion, **(b)** *N*-arylation, and **(c)** quinoidal-aromatic conjugation.

2. Results and discussion

2.1. Preparation and characterization of viologen-quinoid conjugates

Scheme 2 illustrates the synthesis of pyridinium-quinoid conjugates starting from AQM ditriflate **1**, which can be synthesized in two steps following a previously reported procedure (Scheme S1) [46]. Its reaction with 4,4'-bipyridine in refluxing MeCN afforded the ionic AQM derivative iAQM-BPY^{2+}. Further reaction of iAQM-BPY^{2+} with ethyl iodide under reflux yielded iAQM-BPY^{4+}-Et in 52% yield. Both iAQM salts have marginal solubility in aqueous solution after exchanging the anions to bromides. In order to increase the aqueous solubility, an additional viologen-based iAQM with ethanol end group, iAQM-BPY^{4+}-EtOH, was obtained from reacting **1** with the monoalkylated bipyridinium **2**, which showed satisfactory solubility in water. All the ionic AQM salts show good solubility in MeCN after exchanging the anions to hexafluorophosphate (PF_6^-).
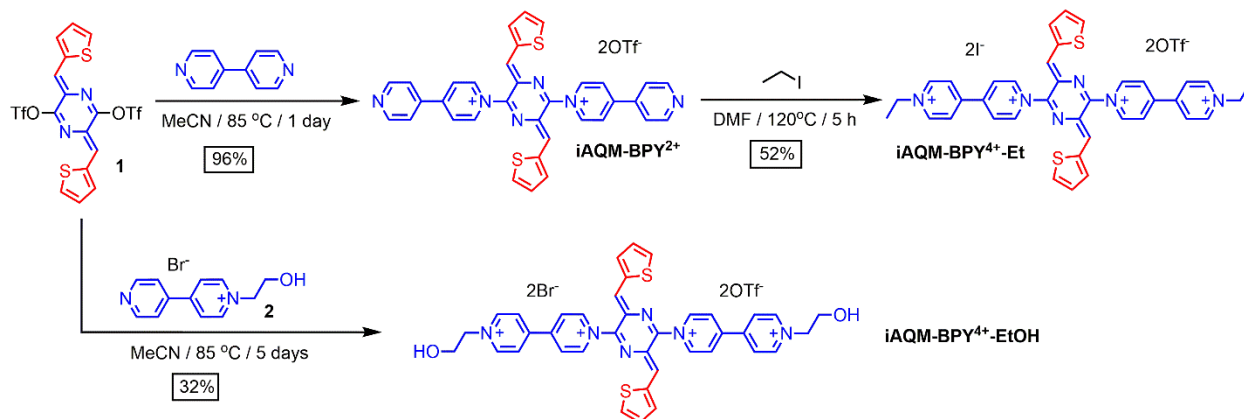
**Scheme 2.** Synthesis of viologen-iAQM conjugates.

The optical and electrochemical properties of those iAQM derivatives (iAQM-BPY^{2+}, iAQM-BPY^{4+}-Et, and iAQM-BPY^{4+}-EtOH) were characterized by UV-Vis and cyclic voltammetry (CV) in MeCN. As shown in Figure 1a, the three iAQM compounds displayed similar absorption features, with two absorption maxima located at around 500 nm and 270 nm, respectively, and a similar absorption edge at 580 nm that corresponds to an optical bandgap of 2.14 eV. The absorption is well extended into the visible region which is in sharp contrast to methyl viologen (MV^{2+}) that has an absorption maximum at 260 nm.
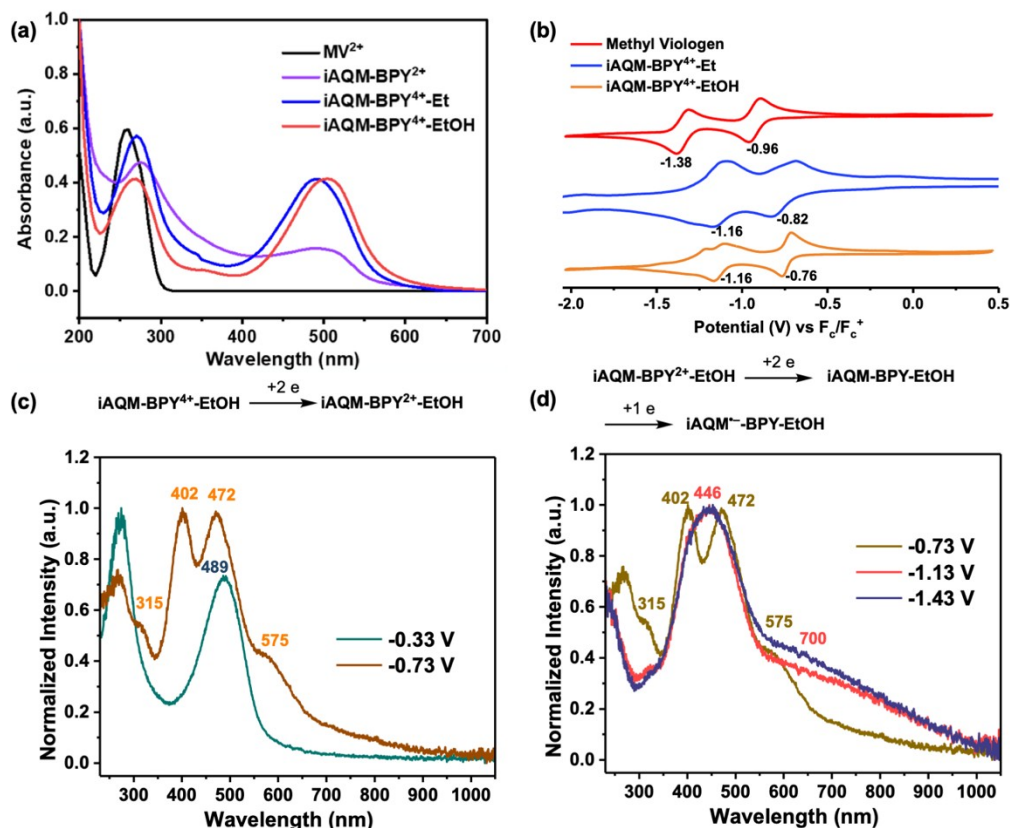
Fig. 1. (**a**) UV-vis spectra of iAQM-BPY^{2+}, iAQM-BPY^{4+}-Et, iAQM-BPY^{4+}-EtOH and MV^{2+} (20.0 μM in MeCN). (**b**) Cyclic voltammograms (1.0 mM in MeCN with 0.1 M NBu$_4$·PF$_6$, scan rate: 100 mV·s^{-1}) of MV^{2+}, iAQM-BPY^{4+}-Et, and iAQM-BPY^{4+}-EtOH. Spectroelectrochemical spectra of iAQM-BPY^{4+}-EtOH showing the absorption changes during (**c**) the first reduction and (**d**) the second and third reduction. The potential is referenced to Fc/Fc$^+$.

The CV studies of both iAQM viologens showed two main redox events, which appeared to be similar to MV^{2+} but with some notable differences (Figure 1b). The CV of iAQM-BPY^{4+}-EtOH showed that the first reduction peak was reversible, while the second reduction peak was broader and appeared as two well-resolved peaks during the anodic scan. The first redox process could be well explained by the degenerate, two one-electron reduction of the dicationic viologen units to their radical cation form (2BPY^{2+}⇔2BPY$^{+\bullet}$, Scheme 3). The broad peak at the higher reductive potential was due to the coalescence of two one-electron reduction of viologen radical cations to their neutral form (2BPY$^{+\bullet}$⇔2BPY^{0}) and the one-electron reduction of the AQM central core (Scheme 3), which could be resolved by differential pulse voltammetry (DPV, Figure S1). The CV profile of iAQM-BPY^{4+}-Et showed similar features to the CV of iAQM-BPY^{4+}-EtOH except that the peaks were broader and less resolved, presumably due to lower solubility caused by less efficient solvation of the reduced species. Compared to MV^{2+}, the first reduction potentials of both iAQM viologens were shifted about 0.2 eV towards a more positive potential, confirming the stronger electron accepting ability endowed by the quinoidal substitution.

Spectroelectrochemical studies were carried out to investigate the reduction induced optical changes of iAQM-BPY^{4+}-EtOH (Figures 1 and S2). When applying a voltage to induced the first reduction within the potential window of -0.4 V and -0.9 V (Figure 1c), both absorption peaks at 270 nm and 500 nm were depleted, accordingly new peaks at 400 nm, 480 nm and 580 nm were formed, which could be assigned to the formation of viologen radicals. The significantly blue shifted absorption peaks compared to that of the MV$^{\bullet+}$ radical was concomitant with the depletion of the absorption of AQM core at 500 nm. Such spectroscopic changes are in accordance with effective delocalization of the unpaired electrons from the two viologen radical cations, through the central quinoidal core, to give the benzylic radicals (Scheme 3). Further increase of the potential led to the disappearance of these fine absorption features and the emergence of a broad peak at 450 nm, together with the appearance of a low-intensity tail reaching 1000 nm (Figure 1d). The former feature is consistent with the full reduction of the viologens to the neutral close-shell state, while the broad near-IR tail is indicative of radical characters due to further reduction of the AQM unit. Such reduction was facilitated by the aromatization of the quinoidal core and the formation of a stable benzylic radical, as illustrated in Scheme 3.
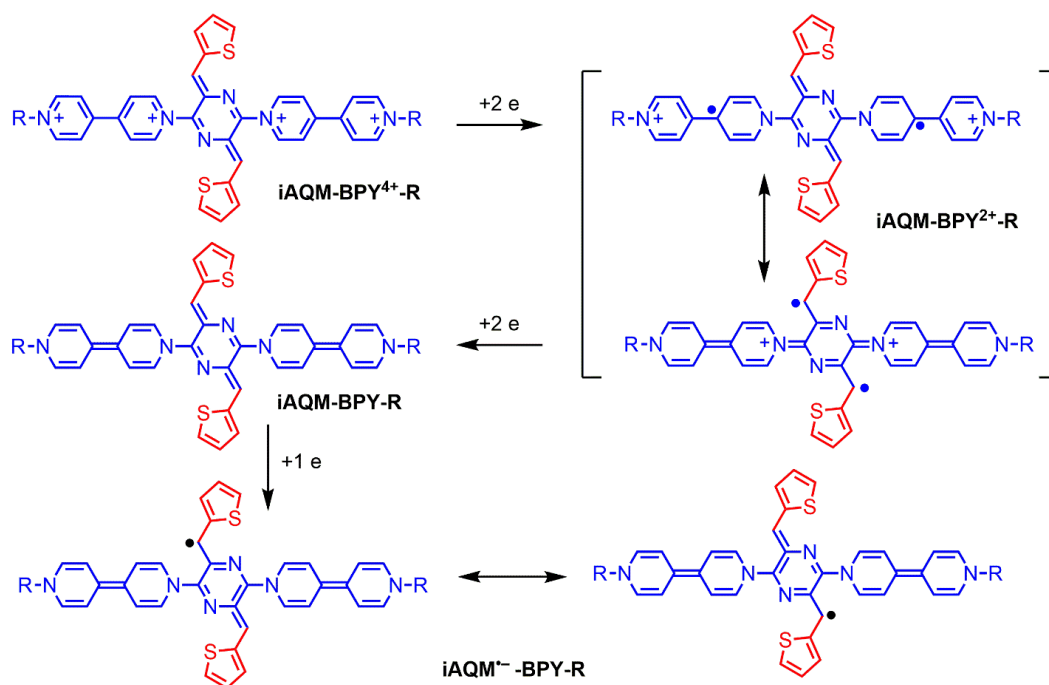

Scheme 3. Illustration of different structures of iAQM viologens at various redox states.

2.2. Theoretical studies on the electronic properties of iAQM-viologen monomer, oligomers and polymers

Density Functional Theory (DFT) calculations were carried out to provide insights on the molecular conformation and electronic properties of the quinoid-viologen conjugates, focusing on the case of iAQM-BPY^{4+}-Et

(See computational details described in Supplemental data). Figure 2a shows some selected dihedral angles for the optimized structure of iAQM-BPY^{4+}-Et in MeCN solution. The thiophene-flanked AQM unit remains coplanar, as was similarly observed in previously reported AQM derivatives, being the dihedral angles $|\alpha| = 2°$. Meanwhile, both viologen pyridinium units are twisted out of plane of the AQM unit, with a dihedral angle $|\beta| = 55°$, which disfavors the electronic conjugation between the two moieties. Such molecular conformation plays a deterministic role on the electronic conjugation and optical properties of iAQM-BPY^{4+}-Et. Figure 2b compares the UV-Vis absorption spectrum with the vertical electronic transitions calculated for this compound. A good match is found between the experimental trace and the vertical bars which represent the calculated electronic transitions. The lowest-energy electronic transition is predicted to be $S_0{\rightarrow}S_3$, mainly involving HOMO and LUMO+2 orbitals (Figure 2c). Both orbitals are mainly distributed on the quinoid unit. Interestingly, LUMO is localized on the viologen units and the transition $S_0{\rightarrow}S_1$ (HOMO$\rightarrow$LUMO) is forbidden (see Table S1 for details).
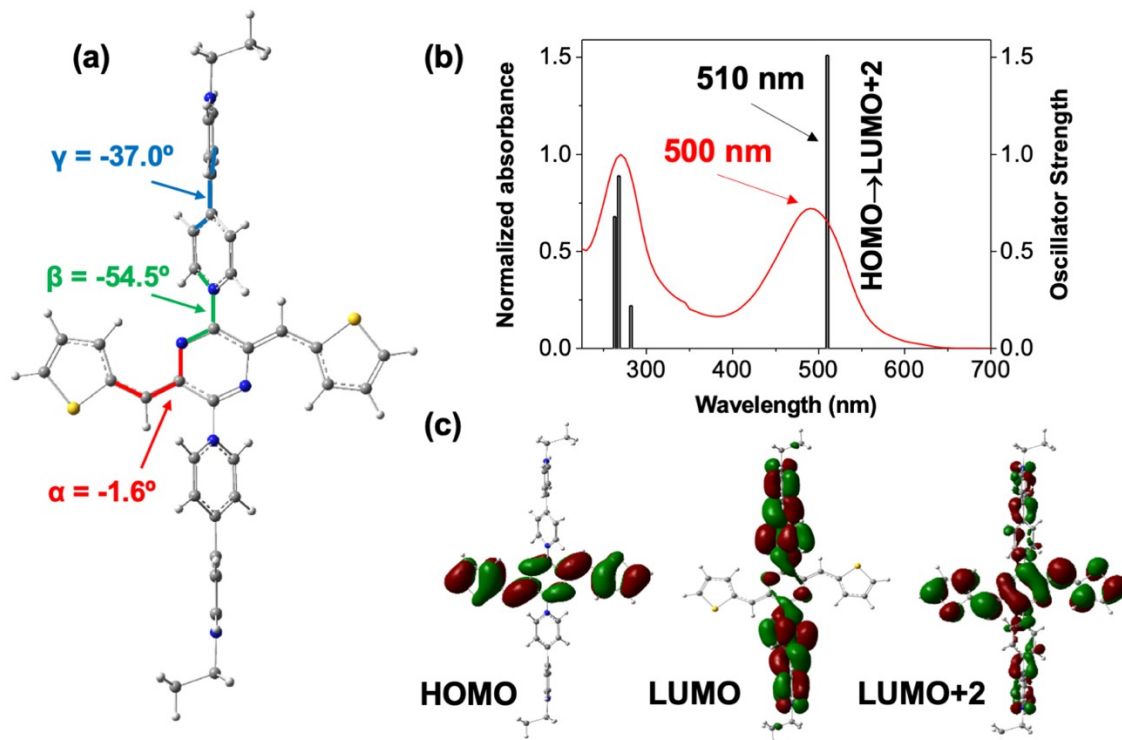

Fig. 2. (a) Molecular geometry calculated for iAQM-BPY^{4+}-Et at the PBE0/6-31G* level of theory in MeCN solution. (b) Experimental spectrum along with calculated vertical electronic transitions for iAQM-BPY^{4+}-Et at the TD-PBE0/6-31G* level of theory (solvent: MeCN). (c) Frontier molecular orbital plots calculated for iAQM-BPY^{4+}-Et (isovalue 0.02 a.u.; PBE0/6-31G*; solvent: MeCN).

Considering our previous experience about narrow bandgap polymers based on iAQM units [47], we decided to explore from a theoretical point of view the effect of the chain length elongation on the electronic and optical properties of quinoid-viologen conjugates. In the absence of experimental data, the results of this theoretical study could justify and encourage experimentalists to approach their synthesis. With this aim in mind, different sized donor-acceptor oligomers were constructed to contain up to six repeat units, with each repeat unit consisting of a quinoid iAQM-BPY^{4+}-Et and an additional thiophene ring. The oligomers were optimized at the PBE0/6-31G* level of theory in MeCN solution. An example of an oligomer with six repeat units is shown in Figure 3a. The quinoidal backbone remains planar upon oligomer elongation, while viologen units are significantly twisted out of plane of the AQM units (see Figure 3b, S11 and S12). The lowest-energy electronic transition was calculated for each oligomer at the TD-PBE/6-31G* level of theory in MeCN solution, from which the evolution of the excitation energy, $E_{(n)}$, upon chain elongation (see Table S2 for details) was analyzed. This analysis allows us to estimate the vertical electronic transition energy for an ideal infinite polymer (E_∞) which is a parameter closely related to the optical bandgap. The values of $E_{(n)}$ were fitted to the equation proposed by Meier et al. [51] where n is the number of repeat units of the oligomer:

$$E_{(n)} = E_\infty + (E_1 - E_\infty) \exp\left[-a\,(n-1)\right]$$

where E_1 is the vertical transition energy of the monomer and *a* is an empirical parameter that describes how fast $E_{(n)}$ saturates to E_∞. As shown in the Figure 3c, a value as small as 0.97 eV was obtained for E_∞ from the fitting. This result indicates the interesting optical properties expected from the donor-acceptor oligomers based on quinoid-viologen conjugates, and points to the possibility of constructing unexplored narrow bandgap redox polymers.
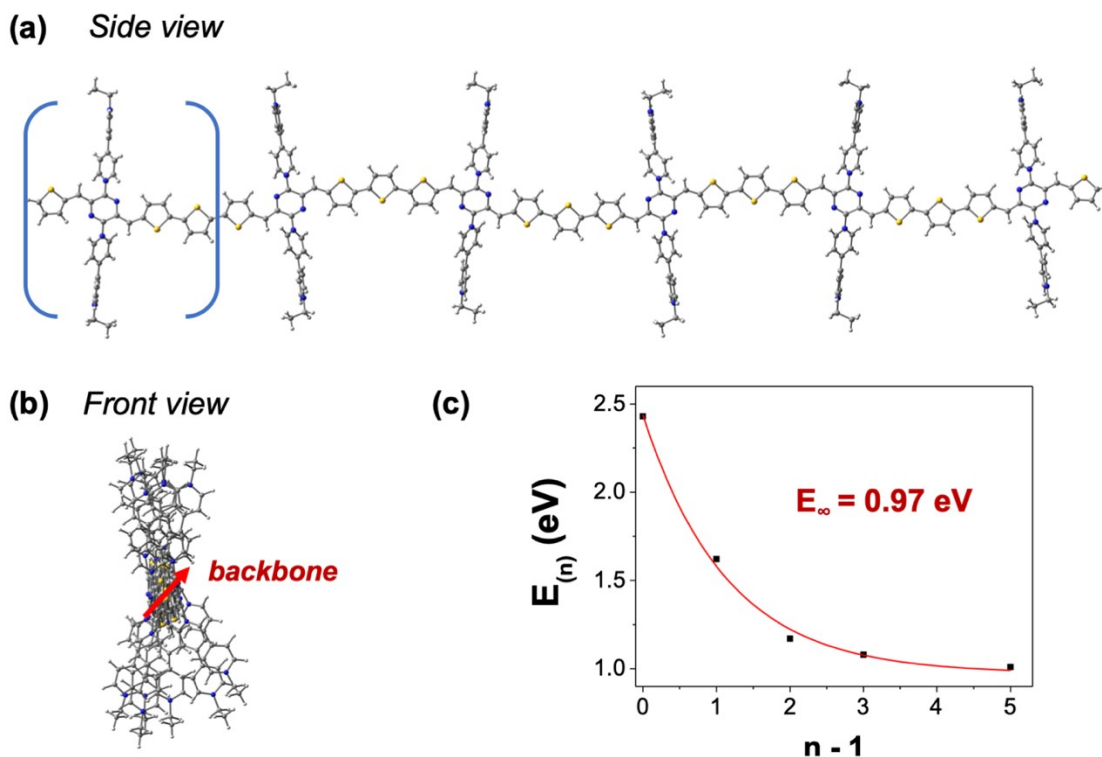
Figure 3. (**a**) Optimized structure of a donor-acceptor hexamer composed of six repeat units that contain an iAQM-BPY[4+]-Et and an additional thiophene unit. A repeat unit is highlighted in the bracket. (**b**) The side view of the optimized structure showing the planar backbone. (**c**) Dependence of the vertical electronic transition energy ($E_{(n)}$) with the chain length and fit to the equation proposed by Meier et al.; E_∞ is the vertical electronic transition energy estimated for an infinite polymer. The calculations were carried out at the PBE0/6-31G* and TD-PBE0/6-31G* levels of theory, in MeCN solution.

2.3. Characterization of the host-guest formation between iAQM-BPY[4+]-EtOH and CBs

Viologens are known to form host-guest complexes with synthetic macrocyclic hosts such as CB[7] and CB[8]. The host-guest binding mode is however highly sensitive to the *N*-substituents of the viologens. Gallopini and coworkers have shown that *N*-tolyl viologen forms a 1:2 complex with CB[7] [52] as opposed to the 1:1 complex from *N*-alkyl viologen and CB[7] [27, 28]. Scherman [50] and coworkers have demonstrated that the electronic effect of the *N*-aryl groups determines the binding stoichiometry between viologens and CB[8], with more electron withdrawing ones forming 1:1 binary complexes while more electron donating ones forming 2:2 quaternary complexes with CB[8]. Given the unusual quinoidal characteristic of the iAQM viologens, it is imperative to study its complexation mode with the CBs to inform the future design of extended hierarchical structures.

iAQM-BPY[4+]-EtOH was chosen to study its supramolecular interactions with the CBs due to its solubility in aqueous solutions. Upon mixing iAQM-BPY[4+]-EtOH with up to two equiv. CB[7] in D_2O (0.2 M NaCl), three out of the four sets of viologen proton resonances became broadened but no significant chemical shift change was observed (Figure S13), suggesting that there was some interaction between CB[7] and the iAQM viologen that hindered the rotation of the viologen units but no inclusion complex was formed. Interestingly, within minutes, red crystals were formed and precipitated from the mixture (Figure 4b), which could be redissolved in D_2O. The ^{1}H NMR spectrum of

the red crystal revealed a 1:2 ratio between iAQM-BPY^{4+}-EtOH and CB[7], suggesting the 1:2 complex with both viologen units being encapsulated (Figure 4e and Figure S14). Characteristic chemical shift changes of the viologen guests also supported its inclusion within the cavity of CB[7]. Out of the four sets of viologen protons, only H$_d$ showed a very small downfield shift (+0.001 ppm) compared to the unbound species, while H$_a$-H$_c$ displayed large upfield chemical shift changes up to 1.5 ppm. Both H$_i$ and H$_j$ methylene protons from the ethanol group underwent an upfield shift of ~0.8 ppm. The large upfield shift was indicative of the relative location of viologen unit within the CB cavity, with the CB host sitting more towards the ethanol end. Furthermore, all of the protons from the iAQM core exhibited a downfield shift, with the H$_e$ vinylidene protons showing the most significant change (+0.5 ppm) while these associated with the thiophene units were smaller (H$_f$: +0.07 ppm; H$_g$: +0.07 ppm; H$_h$: +0.2 ppm). The downfield shift verified the location of AQM protons outside of the CB cavity, with the magnitude in accordance with their relative proximity of the AQM protons with regard to the CB portal. No splitting of CB[7] protons were observed despite their exposure to the asymmetric viologen structure, suggesting that the host-guest complexation is undergoing fast dynamic exchange in the NMR timescale.


Fig. 4. (a) Annotation of the protons of iAQM-BPY^{2+}-EtOH and CB[n]s. **(b)** Optical images showing the CB[7]:iAQM-BPY^{2+}-EtOH crystals rapidly crystallized from the aqueous mixture. ^{1}H NMR spectra showing the host-guest complex formation between iAQM-BPY^{2+}-EtOH and CB[n]s. **(c)** CB[8]:iAQM-BPY^{2+}-EtOH 2:1 complex, **(d)** the pristine iAQM-BPY^{2+}-EtOH, **(e)** CB[7]: iAQM-BPY^{2+}-EtOH complex.

Attempts to characterize the solid-state structure of the complex by single crystal X-ray diffraction led to a partially resolved structure due to the non-ideal crystal quality. Nonetheless, the structure adequately supported the 2:1 complexation between CB[7] and iAQM-BPY^{4+}-EtOH and the relative host-guest arrangement in the solid state

(Figure 5). Both CB[7] macrocycles situate more towards the ethanol ends of the viologens with full enclosure of the corresponding pyridinium units, leaving the other pyridinium units partially extruded from its cavity. While the two viologens remain twisted and rotate out of the plane of the AQM central core, the AQM maintains a coplanar geometry, in keeping with the favourable S•••N interactions [53].
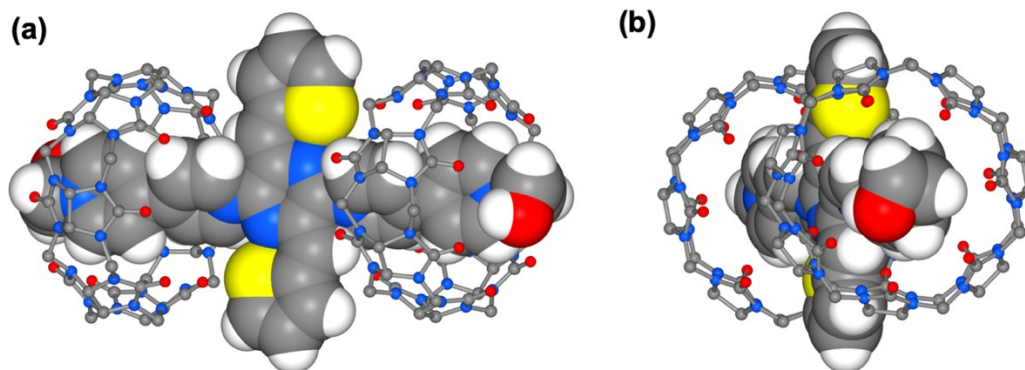
Fig. 5. X-ray structure of the CB[7]:iAQM-BPY^{4+}-EtOH complex, showing the collocation of the iAQM core and the two CB[7] macrocycles in (**a**) front view and (**b**) side view. Gray: carbon, blue: nitrogen; red: oxygen; sulfur: yellow; hydrogen: white.

In the case of binding with CB[8], ^{1}H NMR studies revealed the ready formation of inclusion complex when titrating CB[8] into the aqueous solution of iAQM-BPY^{4+}-EtOH. In contrast to the CB[7] case, while no rapid crystal formation occurred, significant spectroscopic changes were observed (Figure 4c), indicating the instantaneous threading of viologens into the CB[8] cavity, the size of which is sufficiently large that allows the easy passage of the viologen guest. Specifically, upfield shifts of three sets of the viologen bipyridinium protons were observed in the presence of 2 equiv. CB[8], in accordance with their inclusion within CB[8]. Additional amount of CB[8] did not incur further spectroscopic changes, suggesting a complete encapsulation at a 2:1 host-guest ratio (Figure S16). The CB[8]-induced chemical shift changes displayed a very similar pattern to the case of CB[7] (Figure 4c and Figure S17), suggesting a similar binding motif. No 2:2 binding or supramolecular polymer formation was observed despite the bigger cavity of CB[8], presumably disfavored due to stereoelectronic repulsion between the central iAQM units. Furthermore, the addition of an electron rich aromatic species, such as 2,6-dihydroxynaphthalene, into the 1:2 iAQM-BPY^{4+}-EtOH:CB[8] mixture failed to act as a secondary guest to be included in the cavity despite the conceived charge-transfer interaction with iAQM viologen [54].

UV-vis spectroscopic studies were carried out to characterize the complexation between iAQM viologen and the CBs. The main absorption feature of iAQM-BPY^{4+}-EtOH at 500 nm underwent no peak shift, but instead a noticeable intensity decrease was observed after the addition of 2 eq. CB[7] and CB[8] (Figure S18), suggesting that the CB:viologen complexation has minimal impact on the electronic transitions of the AQM component. The similarity between CB[7] and CB[8] complexes also confirmed the 1:1 viologen:CB binding mode. In addition, no charge transfer band was observed when iAQM-BPY^{4+}-EtOH was mixed with 2,6-dihydroxy naphthalene, either in the presence or absence of CB[8]. The lack of charge-transfer complex formation is fully consistent with the NMR results, presumably due to the unfavorable alignment of molecular dipoles and electrostatic interactions.

3. Conclusions

We have demonstrated the first synthesis of viologen-quinoid conjugates using the facile nucleophilic *N*-substitution reaction between pyridyl nitrogen and an AQM ditriflate. The iAQM-viologens show strong electron accepting properties, reversible redox properties, and visible absorption features, matching the characteristics of both the viologen unit and the quinoid unit. Theoretical studies have indicated the possibility of constructing narrow bandgap donor-acceptor polymers based on the iAQM-viologen unit, with a predicted optical bandgap below 1 eV. The supramolecular complexation behavior between iAQM-BPY^{4+}-EtOH with CB[7] and CB[8] were investigated by various spectroscopic methods and/or X-ray crystallography. In both cases, a 2:1 CB:guest complex were favored with each viologen unit being encapsulated by one CB host. The displayed electronic properties and host-guest

complexation behavior distinguish the viologen-quinoid conjugates from the other known *N*-aryl viologens, underscoring the unique role of the quinoid conjugates in imbuing novel properties to the versatile viologen family.

Credit author statement

Ziman Chen: Methodology, Validation, Formal analysis, Investigation, Data curation, Writing-original draft.
Rebecca Khoo: Crystal structure data collection and refinement.
Andrés Garzón-Ruiz: DFT simulation and calculation.
Chongqing Yang: Spectroelectrochemical investigation.
Christopher L. Anderson: Conceptualization.
Amparo Navarro: DFT simulation and calculation.
Xu Zhang: Crystal structure refinement.
Jian Zhang: Crystal structure refinement.
Yongqin Lv: Supervision, Writing-review&editing, Project administration, Funding acquisition.
Yi Liu: Conceptualization, Supervision, Writing-review&editing, Project administration, Funding acquisition.

Declaration of competing interest

The authors declare that they have no known competing financial interests or personal relationships that could have appeared to influence the work reported in this paper.

Acknowledgements

Appendix A. Supplementary data

Supplementary data to this article can be found online at xxx.

Data availability

The processed data of X-ray crystallography are available to download from
https://data.mendeley.com/datasets/zdw53c4y6d/1

References

[1] J. Ding, C. Zheng, L. Wang, C. Lu, B. Zhang, Y. Chen, M. Li, G. Zhai, X. Zhuang, J. Mater. Chem. A 7 (2019) 23337-23360. https://doi.org/10.1039/C9TA01724K.
[2] L. Striepe, T. Baumgartner, Chem. Eur. J. 23 (2017) 16924-16940. https://doi.org/10.1002/chem.201703348.
[3] W. Wu, J. Luo, F. Wang, B. Yuan, T.L. Liu, ACS Energy Letters 6 (2021) 2891-2897. https://doi.org/10.1021/acsenergylett.1c01146.
[4] Y.J. Jang, S.Y. Kim, Y.M. Kim, J.K. Lee, H.C. Moon, Energy Storage Materials 43 (2021) 20-29. https://doi.org/https://doi.org/10.1016/j.ensm.2021.08.038.
[5] Y.R. In, Y.M. Kim, Y. Lee, W.Y. Choi, S.H. Kim, S.W. Lee, H.C. Moon, ACS Appl. Mater. Interfaces 12 (2020) 30635-30642. https://doi.org/10.1021/acsami.0c05918.

[6] M. Xue, Y. Yang, X. Chi, X. Yan, F. Huang, Chem. Rev. 115 (2015) 7398-7501. https://doi.org/10.1021/cr5005869.

[7] I. Neira, A. Blanco-Gómez, J.M. Quintela, M.D. García, C. Peinador, Acc. Chem. Res. 53 (2020) 2336-2346. https://doi.org/10.1021/acs.accounts.0c00445.

[8] C. Cheng, P.R. McGonigal, S.T. Schneebeli, H. Li, N.A. Vermeulen, C. Ke, J.F. Stoddart, Nat. Nanotechnol. 10 (2015) 547-553. https://doi.org/10.1038/nnano.2015.96.

[9] B. Odell, M.V. Reddington, A.M.Z. Slawin, N. Spencer, J.F. Stoddart, D.J. Williams, Angew. Chem. Int. Ed. 27 (1988) 1547-1550. https://doi.org/10.1002/anie.198815471.

[10] V. Balzani, M. Gómez-López, J.F. Stoddart, Acc. Chem. Res. 31 (1998) 405-414. https://doi.org/10.1021/ar970340y.

[11] D.B. Amabilino, J.F. Stoddart, Chem. Rev. 95 (1995) 2725-2828. https://doi.org/10.1021/cr00040a005.

[12] M. Frasconi, I.R. Fernando, Y. Wu, Z. Liu, W.-G. Liu, S.M. Dyar, G. Barin, M.R. Wasielewski, W.A. Goddard, J.F. Stoddart, J. Am. Chem. Soc. 137 (2015) 11057-11068. https://doi.org/10.1021/jacs.5b05618.

[13] R.G.E. Coumans, J.A.A.W. Elemans, A.E. Rowan, R.J.M. Nolte, Chem. Eur. J. 19 (2013) 7758-7770. https://doi.org/10.1002/chem.201203983.

[14] L.M. Klivansky, G. Koshkakaryan, D. Cao, Y. Liu, Angew. Chem. Int. Ed. 48 (2009) 4185-4189. https://doi.org/10.1002/anie.200900716.

[15] C.C. Carmona-Vargas, N. Giuseppone, Chem 7 (2021) 11-13. https://doi.org/10.1016/j.chempr.2020.12.008.

[16] K. Cai, L. Zhang, R.D. Astumian, J.F. Stoddart, Nature Reviews Chemistry 5 (2021) 447-465. https://doi.org/10.1038/s41570-021-00283-4.

[17] Y. Qiu, B. Song, C. Pezzato, D. Shen, W. Liu, L. Zhang, Y. Feng, Q.-H. Guo, K. Cai, W. Li, H. Chen, T. Nguyen Minh, Y. Shi, C. Cheng, R.D. Astumian, X. Li, J.F. Stoddart, Science 368 (2020) 1247-1253. https://doi.org/10.1126/science.abb3962.

[18] C. Barnes Jonathan, C. Fahrenbach Albert, D. Cao, M. Dyar Scott, M. Frasconi, A. Giesener Marc, D. Benítez, E. Tkatchouk, O. Chernyashevskyy, H. Shin Weon, H. Li, S. Sampath, L. Stern Charlotte, A. Sarjeant Amy, J. Hartlieb Karel, Z. Liu, R. Carmieli, Y. Botros Youssry, W. Choi Jang, M.Z. Slawin Alexandra, B. Ketterson John, R. Wasielewski Michael, A. Goddard William, J.F. Stoddart, Science 339 (2013) 429-433. https://doi.org/10.1126/science.1228429.

[19] S.P. Gromov, A.I. Vedernikov, E.N. Ushakov, M.V. Alfimov, Russ. Chem. Bull. 57 (2008) 793-801. https://doi.org/10.1007/s11172-008-0118-4.

[20] K. Takahashi, Chem. Rev. 98 (1998) 2013-2034. https://doi.org/10.1021/cr9700235.

[21] S.J. Barrow, S. Kasera, M.J. Rowland, J. del Barrio, O.A. Scherman, Chem. Rev. 115 (2015) 12320-12406. https://doi.org/10.1021/acs.chemrev.5b00341.

[22] K. Kim, Chem. Soc. Rev. 31 (2002) 96-107. https://doi.org/10.1039/A900939F.

[23] Y.H. Ko, E. Kim, I. Hwang, K. Kim, Chem. Commun. (2007) 1305-1315. https://doi.org/10.1039/B615103E.

[24] L. Isaacs, Acc. Chem. Res. 47 (2014) 2052-2062. https://doi.org/10.1021/ar500075g.

[25] Y. Wu, L. Shangguan, Q. Li, J. Cao, Y. Liu, Z. Wang, H. Zhu, F. Wang, F. Huang, Angew. Chem. Int. Ed. 60 (2021) 19997-20002. https://doi.org/10.1002/anie.202107903.

[26] Y. Han, Z. Meng, Y.-X. Ma, C.-F. Chen, Acc. Chem. Res. 47 (2014) 2026-2040. https://doi.org/10.1021/ar5000677.

[27] H.-J. Kim, W.S. Jeon, Y.H. Ko, K. Kim, Proc. Natl. Acad. Sci. U. S. A. 99 (2002) 5007. https://doi.org/10.1073/pnas.062656699.

[28] W. Ong, M. Gómez-Kaifer, A.E. Kaifer, Org. Lett. 4 (2002) 1791-1794. https://doi.org/10.1021/ol025869w.

[29] Y.H. Ko, I. Hwang, H. Kim, Y. Kim, K. Kim, Chem. Asian J. 10 (2015) 154-159. https://doi.org/10.1002/asia.201402988.

[30] N. Hickey, B. Medagli, A. Pedrini, R. Pinalli, E. Dalcanale, S. Geremia, Cryst. Growth Des. 21 (2021) 3650-3655. https://doi.org/10.1021/acs.cgd.1c00463.

[31] X. Xiao, N. Sun, D. Qi, J. Jiang, Polym. Chem. 5 (2014) 5211-5217. https://doi.org/10.1039/C4PY00512K.

[32] M. Olesińska, G. Wu, S. Gómez-Coca, D. Antón-García, I. Szabó, E. Rosta, O.A. Scherman, Chem. Sci. 10 (2019) 8806-8811. https://doi.org/10.1039/C9SC03057C.

[33] Y.H. Ko, K. Kim, J.-K. Kang, H. Chun, J.W. Lee, S. Sakamoto, K. Yamaguchi, J.C. Fettinger, K. Kim, J. Am. Chem. Soc. 126 (2004) 1932-1933. https://doi.org/10.1021/ja031567t.

[34] S.-Y. Kim, Y.H. Ko, J.W. Lee, S. Sakamoto, K. Yamaguchi, K. Kim, Chem. Asian J. 2 (2007) 747-754. https://doi.org/10.1002/asia.200700043.

[35] L. Zhang, T.-Y. Zhou, J. Tian, H. Wang, D.-W. Zhang, X. Zhao, Y. Liu, Z.-T. Li, Polym. Chem. 5 (2014) 4715-4721. https://doi.org/10.1039/C4PY00139G.

[36] J. Tian, Z.-Y. Xu, D.-W. Zhang, H. Wang, S.-H. Xie, D.-W. Xu, Y.-H. Ren, H. Wang, Y. Liu, Z.-T. Li, Nat. Commun. 7 (2016) 11580. https://doi.org/10.1038/ncomms11580 https://www.nature.com/articles/ncomms11580#supplementary-information.

[37] D.-W. Zhang, J. Tian, L. Chen, L. Zhang, Z.-T. Li, Chem. Asian J. 10 (2015) 56-68. https://doi.org/10.1002/asia.201402805.

[38] L. Chen, X. Zhu, Y. Zhang, G. Gao, W. Xue, S. Zhang, X. Wang, Q. Zhang, X. He, J. Mater. Chem. A 9 (2021) 18506-18514. https://doi.org/10.1039/D1TA03784F.

[39] G. Li, L. Xu, W. Zhang, K. Zhou, Y. Ding, F. Liu, X. He, G. He, Angew. Chem. Int. Ed. 57 (2018) 4897-4901. https://doi.org/10.1002/anie.201711761.

[40] M. Huang, S. Hu, X. Yuan, J. Huang, W. Li, Z. Xiang, Z. Fu, Z. Liang, Adv. Funct. Mater. n/a (2022) 2111744. https://doi.org/10.1002/adfm.202111744.

[41] C. Reus, M. Stolar, J. Vanderkley, J. Nebauer, T. Baumgartner, J. Am. Chem. Soc. 137 (2015) 11710-11717. https://doi.org/10.1021/jacs.5b06413.

[42] W. Ma, L. Xu, S. Zhang, G. Li, T. Ma, B. Rao, M. Zhang, G. He, J. Am. Chem. Soc. 143 (2021) 1590-1597. https://doi.org/10.1021/jacs.0c12015.

[43] Y. Alesanco, A. Viñuales, G. Cabañero, J. Rodriguez, R. Tena-Zaera, ACS Appl. Mater. Interfaces 8 (2016) 29619-29627. https://doi.org/10.1021/acsami.6b11321.

[44] A.J. Greenlee, C.K. Ofosu, Q. Xiao, M.M. Modan, D.E. Janzen, D.D. Cao, ACS Omega 3 (2018) 240-245. https://doi.org/10.1021/acsomega.7b01887.

[45] X. Liu, B. He, A. Garzón-Ruiz, A. Navarro, T.L. Chen, M.A. Kolaczkowski, S. Feng, L. Zhang, C.A. Anderson, J. Chen, Y. Liu, Adv. Funct. Mater. 28 (2018) 1801874. https://doi.org/10.1002/adfm.201801874.

[46] C.L. Anderson, N. Dai, S.J. Teat, B. He, S. Wang, Y. Liu, Angew. Chem. Int. Ed. 58 (2019) 17978-17985. https://doi.org/10.1002/anie.201908609.

[47] C. Anderson, J. Liang, S. Teat, A. Garzon, D.P. Nenon, A. Navarro Rascón, Y. Liu, Chem. Commun. 56 (2020) 4472-4475. https://doi.org/10.1039/D0CC00916D.

[48] C.L. Anderson, J. Liang, S.J. Teat, A. Garzón-Ruiz, D.P. Nenon, A. Navarro, Y. Liu, Chem. Commun. 56 (2020) 4472-4475. https://doi.org/10.1039/D0CC00916D.

[49] C.L. Anderson, H. Li, C.G. Jones, S.J. Teat, N.S. Settineri, E.A. Dailing, J. Liang, H. Mao, C. Yang, L.M. Klivansky, X. Li, J.A. Reimer, H.M. Nelson, Y. Liu, Nat. Commun. 12 (2021) 6818. https://doi.org/10.1038/s41467-021-27090-1.

[50] G. Wu, M. Olesińska, Y. Wu, D. Matak-Vinkovic, O.A. Scherman, J. Am. Chem. Soc. 139 (2017) 3202-3208. https://doi.org/10.1021/jacs.6b13074.

[51] H. Meier, U. Stalmach, H. Kolshorn, Acta Polym. 48 (1997) 379-384. https://doi.org/10.1002/actp.1997.010480905.

[52] M. Freitag, L. Gundlach, P. Piotrowiak, E. Galoppini, J. Am. Chem. Soc. 134 (2012) 3358-3366. https://doi.org/10.1021/ja206833z.

[53] X. Liu, B. He, C.L. Anderson, J. Kang, T. Chen, J. Chen, S. Feng, L. Zhang, M.A. Kolaczkowski, S.J. Teat, M.A. Brady, C. Zhu, L.-W. Wang, J. Chen, Y. Liu, J. Am. Chem. Soc. 139 (2017) 8355-8363. https://doi.org/10.1021/jacs.7b04031.

[54] U. Rauwald, F. Biedermann, S. Deroo, C.V. Robinson, O.A. Scherman, J. Phys. Chem. B 114 (2010) 8606-8615. https://doi.org/10.1021/jp102933h.